

## **A Comparative Investigation of Sintering Methods for Polymer 3D Printing Using Selective Separation Shaping (SSS)**

H. Nouri\*, B. Khoshnevis\*

\*Department of Industrial and Systems and Engineering, University of Southern California, Los Angeles  
California, 90089

### **Abstract**

Selective Separating Shaping (SSS) is a novel additive manufacturing process which is capable of processing polymeric, metallic, ceramic and cementitious materials. In earlier experiments, the capabilities of SSS in fabrication of metallic, ceramic, cement-based and polymeric parts have been demonstrated. The focus of this research has been on exploration of sintering methods in SSS for successful fabrication of polymeric parts. The SSS machine has been used to build specimens made of polyamide (PA6) material. Bonds between layers under two different thermal sintering methods are investigated to achieve better control over shrinkage and maintain effective binding between layers. ImageJ platform and binary surface plots have been used for image processing and evaluating final porosity under each heating mechanism. Further investigations are carried out on properties of the base materials and the choice of sintering mechanism to further improve resolution of final parts.

### **Introduction**

Although AM has developed rapidly and is receiving increasing attention, it is still in early development stage and still significant amount of improvements are expected for AM machines to become mainstream manufacturing equipment. Improvements are expected in the following direction: i. Increasing speed of printing by maintaining quality of printed parts, ii. Online monitoring of process parameters and in-situ sensing techniques to identify deviations and correct them during the process, iii. Apply new materials with desired chemical properties and microstructures. iv. Reducing waste material and further research on reusing recycled materials. v. Fabrication of multi-functional parts and control of material properties and their performance. vi. New AM technologies which can process a wider range of materials in a single platform without a need for retooling. To further expand application of AM to functional engineering parts rather than prototypes, several challenges need to be addressed. There is high demand for a technology that reduces time-to-market and can produce lower cost parts while maintaining high quality. Additionally, a machine with the flexibility in applying multiple classes of material can be more affordable for a firm than multiple machines that each process a certain class of materials. Selective Separation Shaping (SSS) was developed with the goal of fabricating low cost, high resolution parts in a single multi-material platform. This process is not only limited to small scale fabrications, but it also has potential for fabricating on demand large scale structures. For polymeric part fabrication, due to the operation principle in SSS (printing on the boundaries instead of the part body), this process can compete with other processes such as FDM and SLS in printing speed. Multiple nozzles can print at once on the platform without interfering with one another to build multiple objects simultaneously. Compared to other powder-based polymer processes, the end-user product cost will be low as this process does not require laser scanning. The separating material can be purchased at low cost. Additionally, a variety of polymers can be applied to the machine and be tested in powder form. Table 1 summarizes the AM 3D printing fabrication methods for polymer fabrication.

**Table 1. AM methods for fabrication of polymer part geometry creation methods**

<b>AM technology</b>	<b>3D printing method</b>
SLA	UV light beam/Laser
SLS	Laser
FDM	Extrusion
3DP	Binder
DLP	Digital projector screen
DMLS	Laser
SHS	Heat
SLM	Laser
SIS	Separator deposition (Liquid)
SSS	Separator deposition (Solid)

In earlier experiments [1], sample polymer parts with multiple overlapping layers were fabricated by SSS using Copolyamide and Vestamelt 171. Table 2 shows a summary of optimum process parameters used.

**Table 2. Summary of process parameters**

<b>Properties</b>	<b>Description</b>
Thickness of each layer	0.09 to 0.25 mm
Sintering speed	8.3 mm/sec
Sintering temperature	65-70 C
Printing speed	32 sec/layer
Average wait time between layers	12 Sec
Build tank temperature	48 to 60 C
Platform temperature	54 C
Chamber temperature	30 C
Type of polymers	Nylon 6,6
Powder size range	90 to 250 micrometers
S-powder size range	25 to 45 micrometers

Previous SSS research has offered insight into many unknown parameters in the SSS process [2-5]. Zhang et al focused on high temperature sintering material and successfully fabricated metal and ceramic parts. However, bulk sintering approach used in SSS for metal and ceramic has limitations and is not applied to polymers. Therefore, layer by layer sintering approaches need to be carefully studied and implemented.

### **Weak bonding between layers**

One of the key factors in successful fabrication of polymeric parts with SSS is effective sintering of layers. Increasing layer thickness can result in inadequate transfer of heat energy for diffusing successive layers. Figure 1 shows poor bonding between layers for 200 micrometers layer thickness. Depending on the thickness of the layer, sintering adjustments should be made to achieve effective bonding between layers.



**Figure 1. Partially sintered sample with weak bonding between layers**

### **Cumulative heating and warpage**

Depending on the properties of base material and sintering and cooling temperatures and rates, warpage of the layers can occur as shown in Figure 2. Also, as the number of layers increases this phenomenon becomes more significant. Warpage can occur by penetration of heat into previously sintered layers resulting in over-sintering. Moreover, depending on the melting temperature ( $T_m$ ) and crystallization temperature ( $T_c$ ) this warpage can be eliminated in polyamide samples with smaller window between  $T_m$  and  $T_c$  [6-8].



**Figure 2. Warpage caused by cumulative heating**

Non-uniform heating and cooling can be other reasons for layer warpage. Therefore, attempt is made to keep the temperature inside the chamber at a constant level and to pre-heat the platform before printing starts.

### **Shift between layers**

In successive deposition of layers, it is very important to have control over uniformity in the deposition of B-powder over sintered layer to avoid any displacement of previous layer. Shift between layers is one of the main causes for bad quality in the final part. Shifts can be caused by non-uniform sintering of layers, collision of roller with a sintered layer due to inadequate distance from the layer, high friction between roller and surface of powder in build platform, previous layer's warped edge which is easily hit by the roller, software failure, and poor bonding between successive sintered layers. Moreover, B-powder's flowability, particle size and shape as well as roller (or blade) properties such as shape and material, are important factors in successful spreading of powder on previously sintered layer and need to be considered. Finally, Excessive amount of powder fed to the build tank was also observed to be a contributing factor to layer shifting.

### **Shrinkage**

Material shrinkage is one of the main sources of part inaccuracy in AM, primarily caused by thermal phase change of the material during layer formation [9-11]. Proper adjustment of process parameters can severely affect the output quality of the products. In terms of process planning, many research efforts have been dedicated to look for the relationship between the output part quality and the input building process parameters [12-15]. Parametric process optimization is used to improve functional requirement of an additive manufacturing system

such as accuracy by finding the optimal settings of factors such as light intensity of the machine, laser beam width, light exposure duration, scan speed, layer thickness, and so forth. It is crucial to find the appropriate process parameter settings which lead to the best trade-off among part accuracy and manufacturing build time. Several studies have been dedicated to improving part quality by modifying process variables. Sager et al. [16] studied a stereolithography process and investigated the relationship between laser scan speed and surface finish of the final part. He concluded that appropriate laser scan speed leads to a better surface finish of SLA geometries. Raghunath and Pandey [17] investigated the relationship between process parameters and material shrinkage. They examined laser power, beam speed, hatch spacing, part bed temperature and scan length and adopted Taguchi method for analysis of shrinkage. It was concluded that laser power and scan length are found to be most significant process variables influencing shrinkage in the X direction. Senthilkumaran et al. [18] also focused on shrinkage behavior by analyzing the relationship between shrinkage calibration specimen and various building conditions in SLS parts. In order to reach an accurate estimation, layer thickness, laser power, hatch spacing, scanning speed, part bed temperature and scanning mode were studied as the process parameters set in the experiment and beam offset and scanning position were observed to have the major influence on the shrinkage of the part. The focus of this section is to address shrinkage in SSS using process planning and machine parameter setup adjustment. The following section presents the study performed on the strength of the bond between layers using forced convection and the corresponding results.

### **Sintering and coalescence**

Powder sintering refers to a thermal process used to convert a powder volume into a solid object. Polymer sintering is the formation of homogenous mass from the diffusion of smaller particles. Generally, this process is carried out between the glass transition temperature ( $T_g$ ) and melting temperature ( $T_m$ ) of a specific polymer. When polymer particles are heated above  $T_g$ , they form a neck at which polymer chains can interact and diffusion occurs. When the entanglements are fully established, this mass will be at equilibrium [19]. Figure 3 shows growth of the contact neck between powder particles.

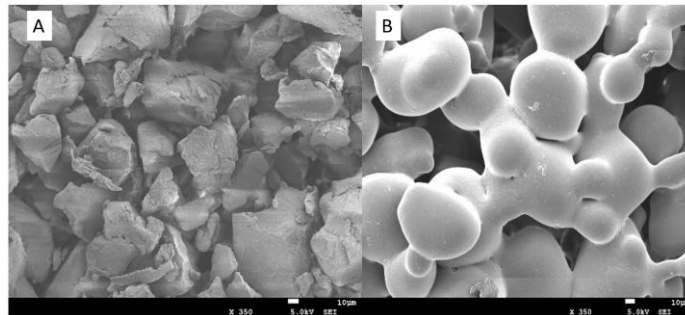


**Figure 3. SEM pictures of powder before(A) and after sintering(B)**

Heat can be transferred between objects by means of radiation, convection, conduction, and microwave [20]. Extensive research work has been done in developing a thermal analysis method for powder metallurgy processes such as Laser sintering [21-23]. Uniform temperature distribution in powder sintering processes can severely affect the final quality of the part. Understanding process mechanisms can significantly contribute to the future development of SSS parts. In the following section, two methods of powder sintering that were examined for SSS of polymeric material are discussed. In the following section two methods of powder sintering that were examined for SSS of polymeric material are discussed.

### **Experimental study**

It is hypothesized that non-deformed inter-layer adhesion can be achieved by convection-based heating at a speed which is at least the same as speed of radiation-based sintering which can produce the same result. Investigation are carried out on base materials properties and the choice of sintering mechanism to further improve mechanical strength and achieve acceptable surface quality. Microanalysis of layers have been

performed to obtain a better understanding of the process. The impact of infrared and convection sintering on samples have been studied. To have a better comparison of the two systems, the amount of heat applied to the powder by each method is determined by measuring the temperature at the point where the powder is sintered. Vestosint material has been used as the base powder for the first set of experiments. Sintering speed is kept constant during all experiments. To study the impact of heat flow on sintered layers, a set of experiments were conveyed with variant distance of convection heater to the powder. Figure 4 represents a binary surface plot of layers sintered under convection heating from distances of 11mm and 4 mm from surface of powder. These distances are selected such that 11 mm is the maximum distance from which sintering is possible and 4 mm is the shortest distance possible to the surface of the powder. These plots are created based on Gaussian light distribution of microscopic images. The heat intensity has been constant in both cases. Although in case b, there is a greater amount of heat flowing inside the powder relative to higher distance exposure, it is observed that decreasing distance of the heater from powder has increased porosity on the layer due to high velocity of the flow. It is observed that in both cases heat penetration depth is relatively high which indicates that in cases where high volume sintering is desirable this approach is suitable (Figure 5).

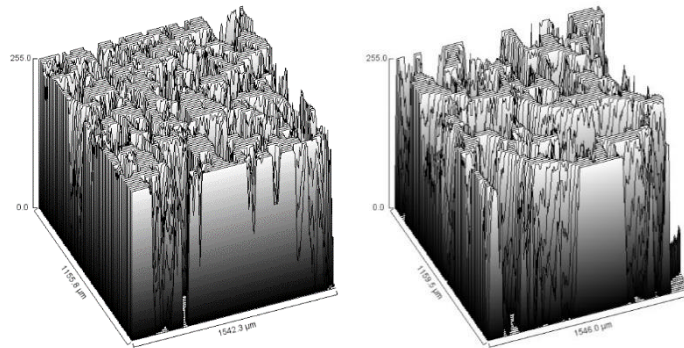


**Figure 4. Surface plot of convection sintering at 11mm distance (left) versus 4 mm (right) from surface layer**

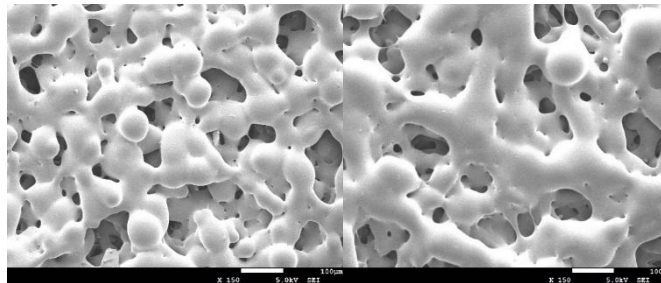


**Figure 5. SEM image of Vestosint at 150 magnitudes sintered at distance 11mm(left) and 4mm (right)**

Increasing the heat intensity under the same condition of distance from surface of powder and flow velocity, results in stronger bonds between particles while maintaining average pore size diameters the same, as opposed to the previous condition in which average pore size was increased. In Figure 6 the surface of Vestosint under low (left) and high (right) heat intensity is shown.

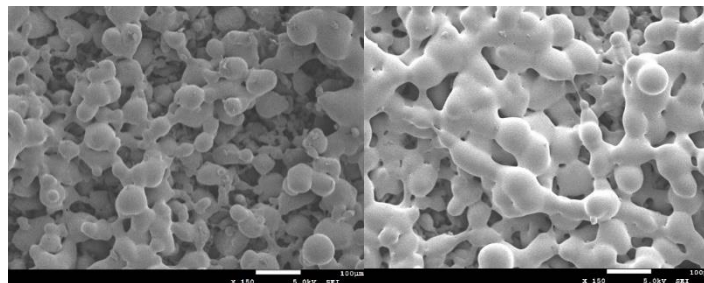


**Figure 6. Surface of Vestosint under in low (left) and high level heat intensity**

In the case of radiation, it is observed that increasing heat intensity from low to high level results in complete coalescence of particles on surface (less porosity on surface); however, does not guarantee bottom particle diffusion (Figure 7).

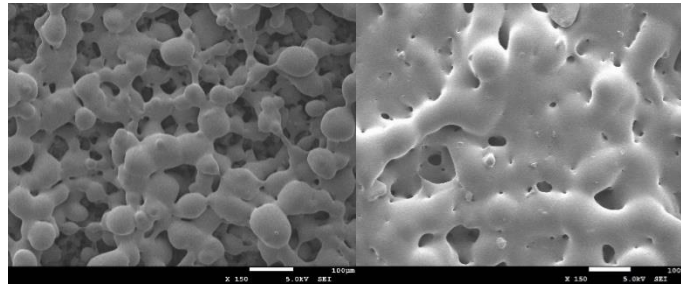


**Figure7. Surface of Vestosint under IR heating in low and high-level heat intensity (4 mm distance)**

In the case of convection sintering, even at high level heat intensity, the energy is absorbed by all particles causing sintering from the bottom up through the whole body. While radiation heat is absorbed in the first layer, any remaining energy is transferred by conduction from top to bottom gradually (Figure 8).

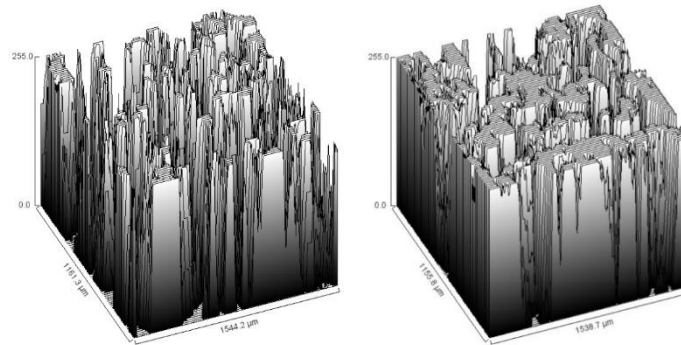


**Figure 8. Surface plot of Vestosint under Radiation heating in low and high level heat intensity (4 mm distance)**

Bright sections on these images are indicative of light transfer through the layers and therefore, sintering level. Similarly, in both cases, bottom layers have a higher level of density as moving up to upper layers shows a decreasing sintering ratio.

### **Selective sintering by forced convective sintering method**

With an understanding of sintering behavior of base material, it was necessary to determine whether or not an effective layer bonding could be achieved through other heat transfer mechanisms. Based on preliminary experiments by linear convective heater discussed in previous section, it was hypothesized that non-deformed inter-layer adhesion can be achieved by convection-based heating at a speed which is at least the same as the speed of radiation-based sintering which can produce the same result. Interlayer adhesion of the top two layers is achieved primarily by conduction of heat from top to lower layer. Conduction takes times, but faster conduction may be achieved with higher radiation intensity but at the expense of layer deformation. More suitable layer shape may be achieved at lower heat delivered over extended time to allow heat conduction from higher to lower layers. However, slow sintering prolongs part fabrication time. Convection-based heating can penetrate heat into top two layers through the pores of the top layer and sinter the two layers simultaneously without the delay that conduction heating would require. The first step was to build parts using this heat transfer approach.

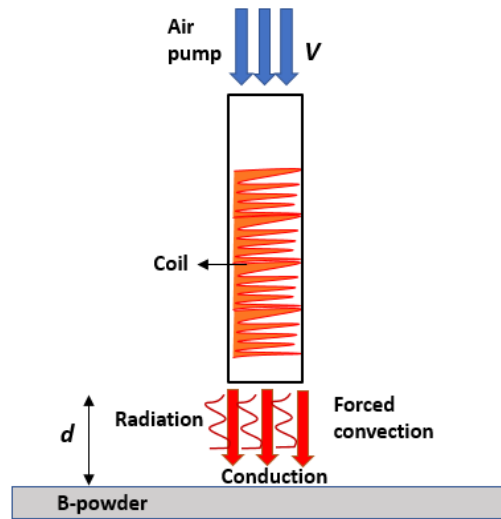


**Figure 9. Schematic of forced convective heater**

A pointwise heater with outer diameter of 6mm and inner diameter of 4 mm was used for experiments. Main components of heater include ceramic tube, kanthal coil, as well as air pump which blows air through the coil along the ceramic tube. A heater cover plate module is installed and is used to block and unblock heat exposure when desired (Figure 9). It was believed that switching heater between on and off state modes on each layer is associated with delays in reaching desired temperature. Thus, weak degree of bonding would be achieved at start points as well as undesired sintered areas following end points.

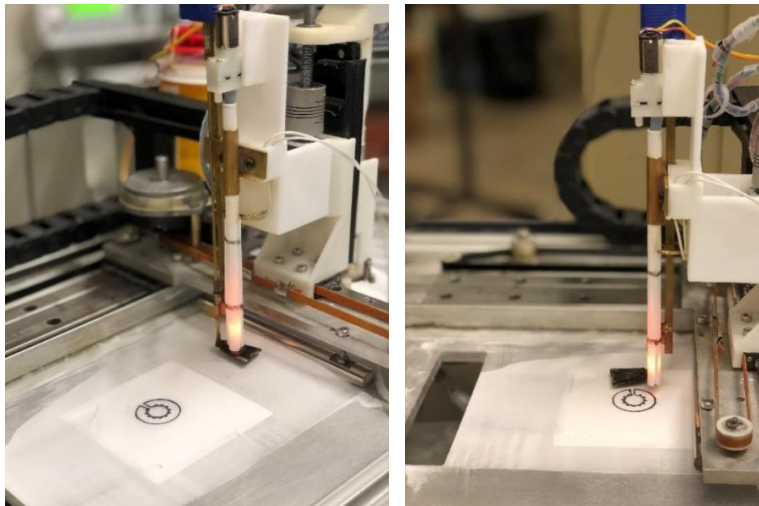


**Figure 10. Demonstration of sintering by forced convective heater**

Upon completion of deposition on a layer, the base plate moves down by an increment equal to half of the layer thickness. Heater is moved over the surface as it can be seen in Figure 10. Sintering starts as the heater moves along the boundary and inner body areas (Figure 11).

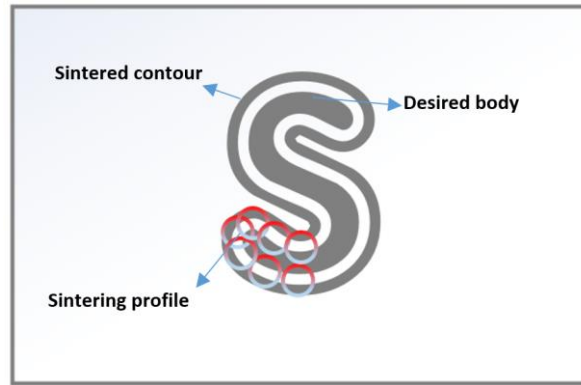


**Figure 11. Sintering profile around the contour of the part**

When sintering is completed, the cover plate module is closed at the endpoint and the base plate moves down by an increment equal to half of layer thickness and the next layer is deposited.

### **DOE for determining significant factors in forced convective sintering**

Design of experiments allows better understanding of relationships between the inputs and the response. A design of experiment technique is used to test the experimental factors at different levels. The motivation to use this approach in this investigation is that it is highly efficient for analyzing process parameters and their interactions effect in convective sintering. This experiment is especially important as it is indicative of the bond formation between successive layers. The design matrix can be seen in Table 4.

**Table 3. Factors**

- 
- A: Distance from powder**
  - B: Heat intensity**
  - C: Air flow**
  - D: Speed of movement**

This experiment was designed for the following purpose: 1. The interaction between distance of the heater from the surface, air pressure of the pump, heat intensity and finally speed of sintering are studied. Optimal setting can be found accordingly for more effective sintering. 2. Effective layer bonding can be examined through evaluation of layer thickness and strength of specimens, 3. Heat transfer mechanisms are compared, and better understanding is obtained. Levels are decided such that, in case of high distance from the surface, it is assumed the main source of sintering is forced convection while in case of low distance and low air pressure, radiation is expected to be the main source. It is important to note that in all cases, there is heat transfer through conduction. However, it is assumed it has been kept equally the same among all runs.



**Table 4. Design matrix (1 at high level and -1 at low level)**

Trial	Distance from powder	Heat intensity	Pump intensity	Speed of movement
1	-1	-1	-1	-1
2	-1	-1	-1	1
3	-1	-1	1	-1
4	-1	-1	1	1
5	-1	1	-1	-1
6	-1	1	-1	1
7	-1	1	1	-1
8	-1	1	1	1
9	1	-1	-1	-1
10	1	-1	-1	1
11	1	-1	1	-1
12	1	-1	1	1
13	1	1	-1	-1
14	1	1	-1	1
15	1	1	1	-1
16	1	1	1	1

For each of the trials shown in the matrix at Table 4, a path with a length of 40 mm and diameter of the heater was sintered. The width of the paths varies depending on distance of the heater from the surface as well as air pressure. Each run was repeated 3 times and to reduce bias experiments were done in a randomized order. The average width, thickness, and tensile strength of each specimen was recorder and are reflected in Table 5.

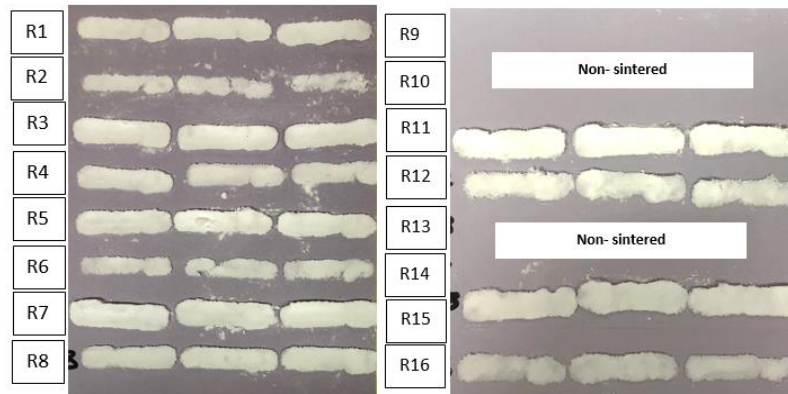


**Figure 12. Sintered lines under different heating conditions**

**Table 5. Average values for three replications**

<b>Trial</b>	<b>Layer thickness (mm)</b>	<b>Tensile strength (N/mm<sup>2</sup>)</b>	<b>Layer width (mm)</b>
<b>1</b>	0.22	13.02	8.77
<b>2</b>	0.12	2.08	6.37
<b>3</b>	0.33	62.08	9.03
<b>4</b>	0.18	9.88	7.60
<b>5</b>	0.28	18.11	7.33
<b>6</b>	0.13	0.00	7.23
<b>7</b>	0.37	51.21	10.07
<b>8</b>	0.23	7.94	8.73
<b>9</b>	0.00	0.00	0.00
<b>10</b>	0.00	0.00	0.00
<b>11</b>	0.25	14.40	8.73
<b>12</b>	0.14	3.57	7.27
<b>13</b>	0.00	0.00	0.00
<b>14</b>	0.00	0.00	0.00
<b>15</b>	0.17	9.00	8.10
<b>16</b>	0.10	8.00	4.93

**Initial experiments to determine factors of importance**

Figure 12 is a visual representation of the level of sintering achievable for the different levels of heat intensity, air pressure, speed and distance of sintering. Comparing values, highest layer thickness and strength was achieved in runs 7 and 3 respectively which suggest high air pressure, low sintering speed. Half-normal plot shown in Figure 13 represent significant factors and interaction in determining layer thickness. As it can be understood, the interaction between air pressure and speed plays a more important role in determining layer thickness rather than interaction between heat intensity and speed.

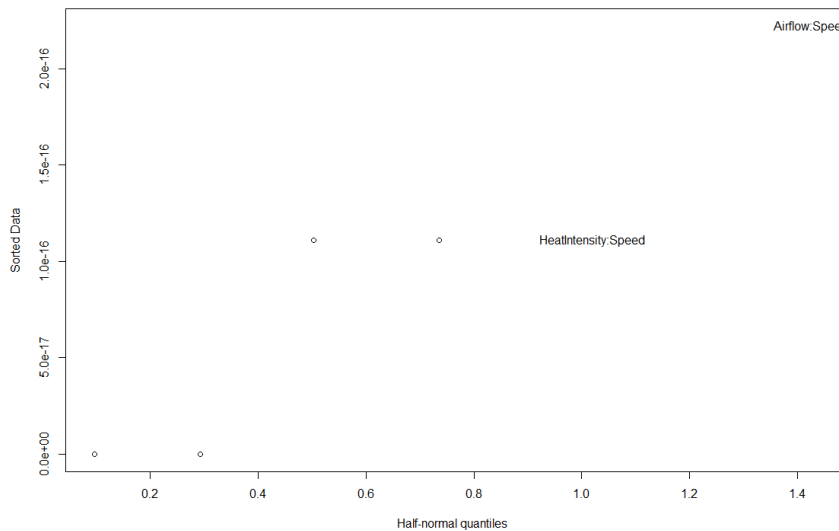


**Figure 13. half normal plot for layer thickness**

It is observed that greater layer thickness shows better heat delivery to bottom layers. Higher penetration of heat through pores is achieved by convective heating. Effective heat transfer results in homogeneous densification and affects microstructure of sintered samples.

### **Discussion**

Suitable layer shape may be achieved at lower heat delivered over extended time to allow heat conduction from higher to lower layers. However, slow sintering prolongs part fabrication time. Convection-based heating can penetrate heat into top two layers through the pores of the top layer and sinter the two layers simultaneously without the delay that conduction heating would require. In our future research, sample parts will be built and tensile tests will be performed to examine mechanical properties of samples.

### **Acknowledgement**

SSS has been conceived and developed in the course of a Phase-II NASA Innovative Advanced Concepts (NIAC) project in relation to the part of the project that concerned landing pad construction.

## References

- [1] Nouri, H., and B. Khoshnevis. "Selective Separation Shaping of Polymeric Parts." In *Solid Freeform Fabrication Symposium*. 2017.
- [2] Khoshnevis, Behrokh, and Jing Zhang. "Selective Separation Sintering (SSS)-An Additive Manufacturing Approach for Fabrication of Ceramic and Metallic Parts with Application in Planetary Construction." AIAA SPACE 2015 Conference and Exposition. 2015.
- [3] Zhang, Jing, and Behrokh Khoshnevis. "Selective Separation Sintering (SSS) A New Layer Based Additive Manufacturing Approach for Metals and Ceramics." *Solid Freeform Fabrication Symposium*. 2015.
- [4] Nouri, Hadis, and Behrokh Khoshnevis. "Study on Inhibition Mechanism of Polymer Parts in Selective Inhibition Sintering Process."
- [5] Khoshnevis, Behrokh, Xiang Gao, Brittany Barbara, and Hadis Nouri. "Selective Separation Shaping (SSS)–Large-Scale Fabrication Potentials." In *Solid Freeform Fabrication Symposium*. 2017.
- [6] Goodridge, R. D., C. J. Tuck, and R. J. M. Hague. "Laser sintering of polyamides and other polymers." *Progress in Materials Science* 57, no. 2 (2012): 229-267.
- [7] Verbelen, Leander, et al. "Characterization of polyamide powders for determination of laser sintering processability." *European Polymer Journal* 75 (2016): 163-174.
- [8] Yusoff, W. A. Y., et al. "Influence of molecular weight average, degree of crystallinity, and viscosity of different polyamide PA12 powder grades on the microstructures of laser sintered part." *MATEC Web of Conferences*. Vol. 26. EDP Sciences, 2015.
- [9] Senthilkumaran, K., Pulak Mohan Pandey, and PV Madhusudan Rao. "Shrinkage compensation along single direction dixel space for improving accuracy in selective laser sintering." *Automation Science and Engineering*, 2008. CASE 2008. IEEE International Conference on. IEEE, 2008.
- [10] Wang, Xiangwei. "Calibration of shrinkage and beam offset in SLS process." *Rapid Prototyping Journal* 5.3 (1999): 129-133.
- [11] Senthilkumaran, K., Pulak Mohan Pandey, and PV Madhusudan Rao. "Shrinkage compensation along single direction dixel space for improving accuracy in selective laser sintering." *Automation Science and Engineering*, (2008). CASE 2008. IEEE International Conference on. IEEE, 2008.
- [12] Dai, K., and L. Shaw. "Distortion minimization of laser-processed components through control of laser scanning patterns." *Rapid Prototyping Journal* 8.5 (2002): 270-276.
- [13] Anitha, R., S. Arunachalam, and P. Radhakrishnan. "Critical parameters influencing the quality of prototypes in fused deposition modelling." *Journal of Materials Processing Technology* 118.1 (2001): 385-388.
- [14] Sood, Anoop Kumar, R. K. Ohdar, and S. S. Mahapatra. "Improving dimensional accuracy of fused deposition modelling processed part using grey Taguchi method." *Materials & Design* 30.10 (2009): 4243
- [15] Górski, Filip, Wiesław Kuczko, and Radosław Wichniarek. "Influence of process parameters on dimensional accuracy of parts manufactured using Fused Deposition Modelling technology." *Advances in Science and Technology–Research Journal* 7.19 (2013).
- [16] Jacobs, Paul F. "The ExpressTool Process." *Rapid Tooling: Technologies and Industrial Applications* (2000): 161.

- [17] Raghunath, N., and Pulak M. Pandey. "Improving accuracy through shrinkage modelling by using Taguchi method in selective laser sintering." *International journal of machine tools and manufacture* 47, no. 6 (2007): 985-995.
- [18] Senthilkumaran, K., Pulak M. Pandey, and P. V. M. Rao. "Influence of building strategies on the accuracy of parts in selective laser sintering." *Materials & Design* 30.8 (2009): 2946-2954.
- [19] Pokluda, Ondřej, Céline T. Bellehumeur, and John Vlachopoulos. "Modification of Frenkel's model for sintering." *AIChE journal* 43.12 (1997): 3253-3256.
- [20] Oghbaei, Morteza, and Omid Mirzaee. "Microwave versus conventional sintering: a review of fundamentals, advantages and applications." *Journal of Alloys and Compounds* 494.1 (2010): 175-189.
- [21] Zeng, Kai, Deepankar Pal, and Brent Stucker. "A review of thermal analysis methods in Laser Sintering and Selective Laser Melting." *Proceedings of Solid Freeform Fabrication Symposium Austin, TX. 2012.*
- [22] Roberts, Ibiye Aseibichin, et al. "A three-dimensional finite element analysis of the temperature field during laser melting of metal powders in additive layer manufacturing." *International Journal of Machine Tools and Manufacture* 49.12 (2009): 916-923.
- [23] Incropera, Frank P., and David P. De Witt. "Fundamentals of heat and mass transfer." (1985).